Biomass Conversion and Biorefinery (2022) 12:515–526
https://doi.org/10.1007/s13399-021-02010-x

ORIGINAL ARTICLE

Drying behavior for *Ocimum basilicum Lamiaceae* with the new system: exergy analysis and RSM modeling

Ahmet B. Demirpolat[1] · Ercan Aydoğmuş[2] · Hasan Arslanoğlu[3]

Received: 13 July 2021 / Revised: 21 September 2021 / Accepted: 29 September 2021 / Published online: 6 October 2021

Abstract

In this study, drying kinetics of Arapgir purple basil leaves under the isothermal and non-isothermal conditions have been investigated. Effective methods were evaluated by drying freshly collected basil leaves in the sun, isothermal, and non-isothermal systems. Energy efficiency was compared in different drying processes by performing exergy analysis in the drying process. It has been observed that the energy consumed and lost especially in the convection drying system (tray dryer) is very high. In the experiments performed in the PID (proportional integral derivative) system, the lowest efficiency was found in the isothermal process. Accordingly, the most suitable system in exergy efficiency was determined as the non-isothermal PID system. Maximum energy loss and minimum exergy efficiency were found at 45 °C temperature and 3.0 m/s airflow rate in the convection drying process. Exergy efficiencies were found to be approximately 4% in the convection tray dryer, 26% in the PID system under isothermal conditions, and 32% in the PID system under non-isothermal conditions. Optimization parameters in the drying process were determined by the response surface methodology (RSM), and the kinetic models were compared with the help of statistical analyses in the experiments. Midilli and Kucuk model has been found as the most compatible kinetic equation with the experimental data. According to this model results, correlation coefficient ($R^2 > 0.990$), sum of squared error ($SSE < 0.005$), chi-square ($\chi^2 < 1 \cdot 10^{-5}$), and root mean square error ($RMSE < 0.003$) values have been evaluated.

Keywords Arapgir basil · Exergy analysis · Drying kinetics · RSM · Shrinkage modeling

Highlights

- According to the exergy results, the efficiency was found to be maximum in the non-isothermal drying performed with the new improved PID system.
- A new model has been developed for the change of surface area in the drying process of the basil leaves.
- The effect of air velocity and temperature on the drying time was determined in the conventional process with RSM.
- The drying behavior of Arapgir basil leaves has been examined with both experimental and theoretical models, and appropriate models are determined by statistical analysis.

✉ Hasan Arslanoğlu
hasan.arslanoglu@comu.edu.tr

Ahmet B. Demirpolat
ahmetb.demirpolat@ozal.edu.tr

Ercan Aydoğmuş
ercanaydogmus@firat.edu.tr

[1] Department of Electronics and Automation, Arapgir Vocational School, Turgut Özal University, Malatya, Turkey

[2] Faculty of Engineering, Department of Chemical Engineering, Fırat University, 23200 Elazığ, Turkey

[3] Faculty of Engineering, Department of Chemical Engineering, Çanakkale Onsekiz Mart University, Çanakkale, Turkey

1 Introduction

Today, some local plants are dried by traditional methods that are widely used in the food industry. For example, the basil plant can be dried under appropriate conditions without losing food and vitamins. Since the drying process causes changes in the appearance, composition, and quality of basil, the drying method applied and the effective parameters should be optimized.

Research examining the drying kinetics of basil leaves was studied in tunnel and tray dryers at temperatures of 55, 60, and 65 °C. Basil leaves have been found to dry faster in the tray dryer than in the tunnel dryer. The effective diffusion coefficient of basil leaves was calculated between 2.65 and $5.69 \cdot 10^{-10}$ m^2/s. The activation energy for the samples dried in both types of dryers was found to be between 33.21 and 9.03 kJ/mol [1].

In an article evaluating the effect of drying on the structural integrity of basil (*Ocimum basilicum* L.), drying in an oven at 45 °C, in the air at room temperature, and freeze-drying was compared. The total amount of volatile components of fresh basil leaves decreased significantly during oven drying and freeze-drying. When the flavor quality has been evaluated among the basil leaves dried with different methods, it was understood that the dried samples most similar to the fresh herb were those that were air-dried at ambient temperature [2].

In the study evaluating the effect of the drying method on aroma compounds of basil (*Ocimum basilicum L.*), convective, vacuum microwave, and combinations have been tried. While the drying kinetics is defined by a two-term exponential model in the convective dryer, it changes linearly up to a critical point and exponentially above this point in the vacuum microwave. To obtain high-quality dried basil, convective pre-drying (40 °C) and post-drying with vacuum microwave (360 W) were determined as the best option (nearly 250 min) [3].

In another research, the necessary optimizations for the protection of the color, aroma, and microbial safety of dried basil have been evaluated. Newly improved drying techniques are discussed to minimize both the valuable compounds and the energy cost of the basil plant. It has been seen that the most economical dryers are the systems improved using solar energy. Studies on the drying of basil and other herbs have been extensively compared in the literature [4, 5].

In the article, the drying behavior of purple basil leaves in the sun, freeze, convective, and microwave oven was investigated, the effects of drying time, speed, and kinetic parameters were investigated. The energy efficiency of different dryers was compared, and a higher drying rate was obtained in microwave drying compared to other methods. When the drying kinetics of basil were examined, it was determined that Henderson and Pabis models were effective in freeze-drying, logarithmic in the sun, Page model in convective and microwave ovens. The effective diffusion coefficient values of purple basil leaves were calculated between $1.62 \cdot 10^{-9}$ and $7.09 \cdot 10^{-8}$ m^2/s [6].

In a study using artificial neural networks and fuzzy logic methods, the drying behavior of basil seed mucilage in an infrared dryer was modeled. The variation of moisture content with drying time has been evaluated depending on the radiation power, mucilage thickness, and surface distance. By using experimental data, it has been determined that artificial neural networks and fuzzy logic simulations gave successful results according to statistical analysis results [7].

Energy savings have been achieved by optimizing processes with the development of new dryers and modification of existing systems [8]. With the advanced exergy analysis, inefficiencies in the energy system were determined quantitatively and qualitatively [9]. To evaluate the performance of the energy system from a thermodynamic and economic point of view, its real potential for improvements and system parameters should be used effectively [10].

In another study investigating the drying kinetics, the mass transfer equation was solved analytically by considering concentration-dependent shrinkage and dehumidification at a constant rate [11]. Besides, in another research conducted by drying foods, the priority is that they do not lose their freshness, color, and vitamin value. Therefore, air temperature, velocity, and system parameters need to be optimized well [12].

In an article that dried basil leaves at 45, 55, and 65 °C air temperatures using different drying methods, the effective diffusion coefficient was calculated between $4.54 \cdot 10^{-10}$ and $1.08 \cdot 10^{-9}$ m^2/s. The activation energy was found to be between 38.54 and 20.32 kJ/mol with the help of the Arrhenius relation [6]. In another research, basil leaves were dried using different techniques at 55, 60, and 65 °C air temperatures, and the drying kinetic models were compared with the help of statistical approaches. It has been determined that basil leaves dry faster in the tray dryer. The logarithmic equation of the kinetic model compatible with the experimental data was obtained at the highest R^2 values. The effective diffusion coefficient calculated for basil leaves was found to be between $2.65 \cdot 10^{-10}$ and $5.69 \cdot 10^{-10}$ m^2/s. The activation energy calculated using the Arrhenius relationship was found to be between 33.21 and 9.03 kJ/mol [13].

In this research, fresh purple basil leaves grown in Arapgir region were collected and prepared for drying. The new improved PID-controlled drying system and conventional tray dryer were used in the drying process. The parameters affecting the drying kinetics under isothermal and non-isothermal conditions have been investigated. The results obtained in experimental studies have been modeled with theoretical equations. Based on energy efficiency, the drying systems were compared by performing an exergy analysis.

2 Materials and methods

2.1 Materials

Arapgir purple basil was procured in the field located at the north 38° 55′ 24.5″ latitude and east 38° 32′ 51.2″ longitude coordinates in the Arapgir district of Malatya province. The basil leaves collected in Arapgir region shown in Fig. 1 were cleaned and prepared for drying. The drying process was carried out in a tray dryer system (Fig. 2) according to the experimental conditions in Table 1.

2.2 Methods used in experimental study

The drying kinetics of Arapgir basil were investigated in a laboratory environment at 1.5, 2.25, and 3.0 m/s constant air velocities and 25 °C, 35 °C, and 45 °C temperatures in a laboratory environment. Characteristic drying curves were determined in the constant drying speed region under experimental conditions. The enthalpy change was calculated taking into account the inlet and outlet temperatures of the air and the losses in the system. It was determined that there was a constant drying region in the system at approximately 5 to 120 min. It was observed that the enthalpy changes in the drying system decreased after 120 min in the region where drying decreased.

In the PID-controlled drying system in Fig. 3, experimental studies were conducted from 20 to 70 °C at a heating rate of 0.15 and 0.20 °C/min.

2.3 Mathematical modeling of drying kinetics

2.3.1 Convectional drying system

In the mass of the basil leaf (M_T), α_t is defined as the conversion rate at any time, the mass of the sample (M_t) at any time, and (t) time. It is the drying rate (D_r) and drying area (A_s) at any given time. The (i) and (f) symbols used in the model equations represent the initial and final time, respectively.

$$\alpha_t = \left(\frac{M_t - M_f}{M_i - M_f} \right) \tag{1}$$

$$D_r = -\frac{M_T}{A_s} \frac{d\alpha}{dt} \tag{2}$$

$$D_r = -\frac{M_T}{A_s(\alpha_t)} \frac{(\alpha_t - \alpha_{t-1})}{(t_t - t_{t-1})} \tag{3}$$

Moisture content was determined as a function of time and drying rate with the average derivative approach [14]. Shrinkage is the volume reduction that occurs during the drying process of the food, and it can generally be up to 85–90% of the initial volume ($\beta = 0.942$ and $\delta = 0.058$) [15].

$$\frac{V}{V_i} = \beta \left(\frac{\alpha}{\alpha_i} \right) + \delta \tag{4}$$

$$A_s(\alpha_t) = \left(\varphi l^2 + \phi w^2 \right) e^{(\alpha_t - 1)} + \xi \tag{5}$$

Area changes according to time were calculated according to the surface area model developed for the basil leaves. Correlation coefficients were calculated according to the transformation ratio of the leaf with its length (l) and width (w). Shrinkage coefficients ($R^2 = 0.9982$) were found for the length (φ) and width (ϕ) of the leaf. Besides, the species correction coefficient (ξ) was added to Eq. 5, since the leaves of various vegetative species show different characteristics [16, 17].

2.3.2 Non-isothermal drying kinetics

Non-isothermal drying kinetics model equations are solved according to the Coats-Redfern method [19, 20]. The activation energy (E), Arrhenius constant (A), and R^2 values were calculated with the help of the models in Eq. 8 and Table 2.

$$\frac{da}{dt} = k(T) f(\alpha) \tag{6}$$

$$k(T) = A exp(-\frac{E}{RT}) \tag{7}$$

$$ln \frac{g(\alpha)}{T^2} = ln \frac{AR}{E\delta} - \frac{E}{RT} \tag{8}$$

Activation energy and other correlation coefficients were calculated according to the Coats-Redfern method with the drying kinetic equations (Eqs. 6, 7, and 8) using the conversion rate which were specified in Eq. 1. In Table 2, drying kinetic models commonly used in the literature for non-isothermal conditions are given.

2.4 Exergy analysis

Dehumidification, enthalpy change, maximum enthalpy value, time, and energy amount during drying are very

Fig. 1 Image of Arapgir basil (*Ocimum basilicum* L.) leaves growing in Eastern Anatolia Region

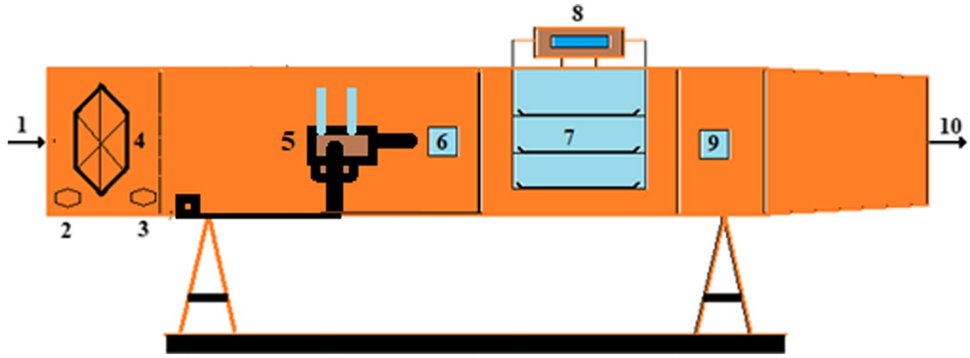

Fig. 2 Forced convection insulated tray drier: Inflow air (1), air flow control (2), temperature controller (3), heater fun (4), temperature measurement system (5), first region (6), porous metal trays (7), digital mass scale (8), second region (9), and outflow air (10)

important for drying thermodynamics. In the drying process, exergy analysis is carried out according to the second law of thermodynamics, in which the quality of energy is important as well as the quantity and this process takes place in a direction that reduces the energy quality [21, 22].

According to the principle of conservation of energy in a system, the total amount of energy entering and leaving is in equilibrium. Equation 9 is written for the energy balance in the drying system according to this principle. Here, $\dot{Q}$ is the heat energy input, $\dot{m}$ is the mass flow, and h is the enthalpy.

$$\dot{Q} = \sum \dot{m}_{out}h_{out} - \sum \dot{m}_{in}h_{in} \quad (9)$$

Equation 10 is obtained if the forces entering and leaving the system are constant.

$$\dot{Q} = \dot{m}\left(h_{out} - h_{in}\right) = \dot{m}\Delta h \quad (10)$$

C_p is the specific heat, T is the temperature, λ is the latent heat of evaporation, and w is the humidity. The enthalpy of the drying air is calculated as follows: Eq. 11

$$h = C_{p,air}T_{air} + \lambda w \quad (11)$$

The second law of thermodynamics states that some losses can occur in a system due to irreversibility. In the drying process in this study, input, output, and losses in the system for exergy analysis were calculated. The energy is given to the system in a steady-state; the energy coming out of the system and other losses have been determined.

Equation 12 can be used to calculate exergy inputs and outputs at inlet and outlet temperatures, respectively, where E_α is exergy and ∞ indicates the ambient condition. Also, the exergy loss during the process is determined using the following expression.

Table 1 RSM study plan designed for the tray dryer experiment system

Experiments (Exp) No	Temperature °C	Airflow rate (m/s)	Drying time (min)
1	35	2.25	294
2	35	3	265
3	42	1.72	252
4	42	2.78	211
5	45	2.25	206
6	35	1.5	323
7	25	2.25	382
8	28	1.72	377
9	28	2.78	336
10	35	2.25	293
11	35	2.25	295
12	35	2.25	292
13	35	2.25	296

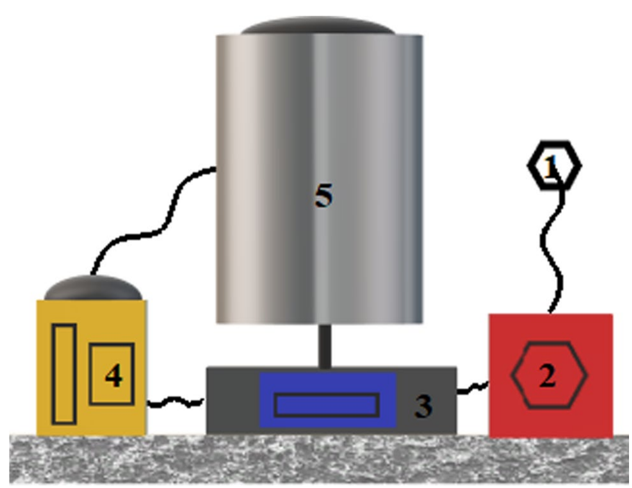

Fig. 3 PID-controlled isothermal and non-isothermal drying system: Electrical source (1), potentiometer (2), mass scale (3), temperature controller (4), and insulated drying the system (5)

Table 2 The non-isothermal drying kinetics models used for Arapgir basil [18]

No	Kinetic models	$f(\alpha)$	$g(\alpha)$
1	Avrami-Erofe	$2(1-\alpha)[-ln(1-\alpha)]^{1/2}$	$[-ln(1-\alpha)]^{1/2}$
2	Avrami-Erofe	$3(1-\alpha)[-ln(1-\alpha)]^{2/3}$	$[-ln(1-\alpha)]^{1/3}$
3	Avrami-Erofe	$4(1-\alpha)[-ln(1-\alpha)]^{3/4}$	$[-ln(1-\alpha)]^{1/4}$
4	One-dimensional diffusion	$1/(2\alpha^{-1})$	α^2
5	Two-dimensional diffusion	$[-ln(1-\alpha)]^{-1}$	$[(1-\alpha)ln(1-\alpha)]+\alpha$
6	Three-dimensional diffusion	$(3/2)(1-\alpha)^{2/3}[1-(1-\alpha)^{1/3}]^{-1}$	$[1-(1-\alpha)^{1/3}]^2$
7	Ginstling-Brounshtein	$(3/2)[(1-\alpha)^{-1/3}-1]^{-1}$	$(1-2\alpha/3)-(1-\alpha)^{2/3}$
8	First order	$(1-\alpha)$	$-ln(1-\alpha)$
9	Second order	$(1-\alpha)^2$	$(1-\alpha)^{-1}-1$
10	Third order	$(1-\alpha)^3$	$[(1-\alpha)^{-2}-1]/2$
11	Parabolic Law	$1/\alpha$	$\alpha^2/2$
12	Holt-Cutler-Wadsword	$1/-ln(1-\alpha)$	$(1-\alpha)ln(1-\alpha)+\alpha$
13	Jander	$(1-\alpha)^{2/3}/[1-(1-\alpha)^{1/3}]$	$3(1-(1-\alpha)^{1/3})^2/2$
14	Zhuravlev-Lesokhin-T	$(1-\alpha)^{5/2}/[1-(1-\alpha)^{1/3}]$	$3[(1-\alpha)^{-1/3}-1]^2/2$
15	Komatsu-Uemuro	$(1+\alpha)^{2/3}/[(1+\alpha)^{1/3}-1]$	$3[(1+\alpha)^{1/3}-1]^2/2$

$$E_\alpha = C_{p,air}\left[\left(T_g - T_\infty\right) - T_\infty \ln\left(\frac{T_g}{T_\infty}\right)\right] \tag{12}$$

$$\sum E_{\alpha,loss} = \sum E_{\alpha,in} - \sum E_{\alpha,out} \tag{13}$$

$$\sum E_{\alpha,loss} = \sum E_{\alpha,in} - \sum E_{\alpha,out} \tag{14}$$

Exergy efficiency (η_α) is defined by the characteristics of the air entering and leaving the system [23, 24].

3 Results and discussion

3.1 Activation energy results and correlation coefficients

The results in Table 3 were found using the models in Table 2 according to the Coats-Redfern method. While examining the drying kinetics of Arapgir basil, the models common in the literature have been preferred [18].

For the model equations in Table 4, statistical analysis was performed, and correlation coefficients, R^2 values, and

Table 3 Drying correlation coefficients of Arapgir basil for two experiments

No	0.20 °C/min			0.15 °C/min		
	A (1/min)	E (kJ/mol)	R^2	A (1/min)	E (kJ/mol)	R^2
1	0.00053	1.88648	0.99513	0.00030	1.73395	0.97654
2	0.00816	2.69922	0.99583	0.00040	2.49584	0.98014
3	0.03227	3.10558	0.99603	0.00145	2.87678	0.98116
4	334.731	6.84945	0.96604	88.8902	6.45367	0.94321
5	1792.47	7.44795	0.98115	408.261	7.01119	0.96195
6	10,164.0	8.27138	0.99395	1736.04	7.75885	0.97849
7	1137.88	7.71458	0.98656	237.108	7.25448	0.96862
8	0.21108	4.32468	0.99639	0.07173	4.01962	0.98301
9	291.405	6.18025	0.94542	41.1815	5.64267	0.94748
10	262,574	8.51667	0.86896	1,169,240	7.67713	0.87856
11	167.360	6.84945	0.96604	44.1832	6.45367	0.94321
12	1483.76	7.44795	0.98115	408.540	7.01119	0.96195
13	1992.13	8.27138	0.99395	260.518	7.75885	0.97849
14	419,189	9.89231	0.98932	302,352	9.55331	0.98237
15	6.65210	6.32413	0.99083	1.93143	5.95331	0.92799

Table 4 Kinetic models used in non-linear regression analysis of the for the basil [6]

Model (Mod)	Model name	Equations
1	Lewis	M_R = exp(-kt)
2	Page	M_R = exp(-kt^n)
3	Modifiye Page	M_R = exp(-(kt)^n)
4	Henderson ve Pabis	M_R = (m)exp(-kt)
5	Logarithmic	M_R = (m)exp(-kt) + n
6	Two term	M_R = (m)exp(-kt) + (n)exp(-zt)
7	Midilli and Kucuk	M_R = (m)exp(-kt^n) + zt
8	Diffusion approach	M_R = (m)exp(-kt) + (1-m) exp(-knt)
9	Verma et al	M_R = (m)exp(-kt) + (1-m) exp(-nt)

error function were calculated, and the results in Table 5 with Table 6 were found.

3.2 Results of statistical analysis

In this section, a statistical comparison has been made with experimental data to investigate the reliability of theoretical equations. By calculating the error functions, the closeness of the most suitable models to the real experimental results was determined. As can be seen in Tables 5 and 6, the models with calculated correlation coefficients have found the most suitable models for high R^2 values and low error functions. In the statistical error analysis examined here, root mean square error (*RMSE*), chi-square (χ^2), and sum of squared error (*SSE*) were performed [25–27].

Table 5 Drying kinetics and statistical analysis for Arapgir basil leaves

Exp	Mod	*k*	*m*	*n*	*z*	R^2	*RMSE*	*SSE*	χ^2
1	1	0.00209				0.89021	0.00916	0.00059	0.00015
	2	0.00023		1.67243		0.98922	0.00287	0.00006	0.00002
	3	0.00672		1.69030		0.98927	0.00286	0.00006	0.00002
	4	0.00283	1.01858			0.97555	0.00432	0.00013	0.00004
	5	0.00032	8.55469	−7.53699		0.97804	0.00410	0.00012	0.00004
	6	0.00283	0.96714	0.05144	0.00282	0.97555	0.00432	0.00013	0.00004
	7	3.66998	38.8209	−0.00486	−0.00385	0.99276	0.00236	0.00004	0.00001
	8	−0.00683	3.71898	1.40819		0.98432	0.00346	0.00008	0.00003
	9	0.00397	1.05914	0.07934		0.99123	0.00259	0.00005	0.00002
2	1	0.00246				0.94741	0.00675	0.00032	0.00008
	2	0.00070		1.38236		0.99189	0.00265	0.00005	0.00002
	3	0.00521		1.38252		0.99132	0.00283	0.00006	0.00002
	4	0.00308	1.01551			0.99937	0.00074	$3.8{\cdot}10^{-6}$	$1.3{\cdot}10^{-6}$
	5	0.00169	1.79738	−0.78249		0.99947	0.00068	$3.2{\cdot}10^{-6}$	$1.1{\cdot}10^{-6}$
	6	0.00308	0.98873	0.02678	0.00307	0.99937	0.00074	$3.8{\cdot}10^{-6}$	$1.3{\cdot}10^{-6}$
	7	−0.00020	1.01373	0.62051	−0.00299	0.99958	0.00067	$1.1{\cdot}10^{-6}$	$0.5{\cdot}10^{-6}$
	8	−0.00428	3.66158	1.52282		0.98341	0.00379	0.00010	0.00003
	9	0.00313	1.01697	0.40903		0.99935	0.00051	$1.8{\cdot}10^{-6}$	$0.6{\cdot}10^{-6}$
3	1	0.00323				0.94267	0.00924	0.00060	0.00015
	2	0.00083		1.41341		0.99255	0.00333	0.00008	0.00003
	3	0.00661		1.41375		0.99201	0.00349	0.00009	0.00003
	4	0.00409	1.02135			0.99883	0.00132	0.00001	$4.1{\cdot}10^{-6}$
	5	0.00101	3.89372	−2.87414		0.99929	0.00103	$7.4{\cdot}10^{-6}$	$2.5{\cdot}10^{-6}$
	6	0.00409	0.98171	0.03964	0.00407	0.99883	0.00132	0.00001	$4.1{\cdot}10^{-6}$
	7	1.01448	2.80267	−0.00168	−0.00396	0.99943	0.00092	$6.0{\cdot}10^{-6}$	$2.0{\cdot}10^{-6}$
	8	−0.00437	3.75613	1.55038		0.98267	0.00508	0.00018	0.00006
	9	0.00409	1.02135	5.40717		0.99883	0.00132	0.00001	$4.1{\cdot}10^{-6}$
4	1	0.00420				0.94290	0.01176	0.00097	0.00024
	2	0.00108		1.41261		0.99293	0.00414	0.00012	0.00004
	3	0.00796		1.41379		0.99235	0.00422	0.00014	0.00004
	4	0.00532	1.02763			0.99924	0.00135	0.00001	$4.3{\cdot}10^{-6}$
	5	0.00136	3.71369	−2.68897		0.99977	0.00074	$3.9{\cdot}10^{-6}$	$1.3{\cdot}10^{-6}$
	6	0.00532	0.94552	0.08211	0.00529	0.99924	0.00135	0.00001	$4.3{\cdot}10^{-6}$
	7	−0.00079	1.02233	0.38361	−0.00498	0.99982	0.00066	$3.1{\cdot}10^{-6}$	$1.0{\cdot}10^{-6}$
	8	0.00544	1.03089	69.4291		0.99966	0.00091	$5.8{\cdot}10^{-6}$	$1.9{\cdot}10^{-6}$
	9	0.00420	0.95712	0.00419		0.94683	0.01198	0.00114	0.00032

Statistical analyses were performed to determine the most suitable models in the non-isothermal experimental studies conducted in the PID controlled system. When the results obtained in the non-isothermal drying were examined in Table 3, it was seen that the R^2 values of models 2, 3, 6, 8, 13, and 14 were higher. In the model equations, activation

Table 6 Correlation coefficients and statistical analysis for Arapgir basil leaves

Exp	Mod	*k*	*m*	*n*	*z*	R^2	*RMSE*	*SSE*	χ^2
5	1	0.00506				0.93721	0.01482	0.00154	0.00038
	2	0.00118		1.44249		0.99260	0.00509	0.00018	0.00006
	3	0.00935		1.44251		0.99205	0.00530	0.00020	0.00006
	4	0.00649	1.03518			0.99897	0.00190	0.00003	0.00001
	5	0.00141	4.31464	− 3.28396		0.99973	0.00097	$6.7 \cdot 10^{-6}$	$2.2 \cdot 10^{-6}$
	6	0.00649	0.97643	0.05874	0.00648	0.99897	0.00190	$2.5 \cdot 10^{-5}$	$8.4 \cdot 10^{-6}$
	7	− 0.00073	1.02793	0.66747	− 0.00611	0.99977	0.00089	$5.5 \cdot 10^{-6}$	$1.8 \cdot 10^{-6}$
	8	− 0.00693	3.66691	1.52282		0.98260	0.00780	0.00043	0.00014
	9	0.00649	1.03518	5.09113		0.99897	0.00190	0.00003	$8.4 \cdot 10^{-6}$
6	1	0.00549				0.94726	0.01429	0.00143	0.00036
	2	0.00158		1.37917		0.99142	0.00576	0.00023	0.00008
	3	0.00977		1.42886		0.99084	0.00596	0.00025	0.00008
	4	0.00689	1.03429			0.99971	0.00106	$7.9 \cdot 10^{-6}$	$2.6 \cdot 10^{-6}$
	5	0.00456	1.49387	− 0.46180		0.99982	0.00084	$5.0 \cdot 10^{-6}$	$1.7 \cdot 10^{-6}$
	6	0.00689	0.94784	0.08645	0.00684	0.99971	0.00106	$7.9 \cdot 10^{-6}$	$2.6 \cdot 10^{-6}$
	7	0.00515	1.03859	0.70742	− 0.00466	0.99988	0.00070	$3.4 \cdot 10^{-6}$	$1.1 \cdot 10^{-6}$
	8	0.00686	3.73849	1.52696		0.98011	0.00878	0.00054	0.00018
	9	0.00549	0.96373	0.00549		0.94726	0.01429	0.00143	0.00048
7	1	0.00678				0.93849	0.01899	0.00253	0.00063
	2	0.00166		1.42899		0.99180	0.00694	0.00034	0.00011
	3	0.01137		1.42960		0.99125	0.00716	0.00036	0.00011
	4	0.00867	1.04628			0.99940	0.00187	0.00003	0.00001
	5	0.00382	2.16489	− 1.12428		0.99978	0.00086	$5.1 \cdot 10^{-6}$	$1.7 \cdot 10^{-6}$
	6	0.00867	1.00260	0.04368	0.00865	0.99940	0.00187	$2.5 \cdot 10^{-5}$	$8.2 \cdot 10^{-6}$
	7	0.00418	1.04470	0.75734	− 0.00608	0.99982	0.00103	$2.4 \cdot 10^{-6}$	$1.6 \cdot 10^{-6}$
	8	− 0.00598	3.81200	1.60703		0.98210	0.01025	0.00073	0.00024
	9	0.00887	1.05180	0.38568		0.99988	0.00085	$5.0 \cdot 10^{-6}$	$1.7 \cdot 10^{-6}$
8	1	0.00760				0.93774	0.02110	0.00312	0.00078
	2	0.00191		1.42244		0.99004	0.00844	0.00050	0.00017
	3	0.01226		1.42315		0.98940	0.00865	0.00052	0.00017
	4	0.00972	1.05171			0.99872	0.00303	0.00006	0.00002
	5	0.00630	1.51895	-0.47170		0.99895	0.00274	0.00005	0.00002
	6	0.00972	0.99126	0.06045	0.00970	0.99872	0.00303	$6.4 \cdot 10^{-5}$	$2.1 \cdot 10^{-5}$
	7	0.00706	1.02573	1.23612	0.00483	0.99928	0.00227	0.00004	0.00001
	8	− 0.00569	3.74349	1.67488		0.97930	0.01217	0.00104	0.00035
	9	0.00991	1.05699	0.41417		0.99909	0.00256	0.00005	0.00002
9	1	0.00868				0.93164	0.02514	0.00443	0.00111
	2	0.00187		1.47015		0.99263	0.00825	0.00048	0.00016
	3	0.01411		1.48894		0.99256	0.00829	0.00048	0.00016
	4	0.01125	1.06244			0.99849	0.00374	0.00010	0.00003
	5	0.00315	3.24844	− 2.19782		0.99980	0.00135	0.00001	$4.3 \cdot 10^{-6}$
	6	0.01125	0.95828	0.10416	0.01124	0.99849	0.00374	$9.8 \cdot 10^{-5}$	$3.3 \cdot 10^{-5}$
	7	0.00644	1.03665	1.18560	0.00119	0.99990	0.00098	$6.7 \cdot 10^{-6}$	$2.2 \cdot 10^{-6}$
	8	0.01174	1.07621	25.4742		0.99966	0.00179	0.00002	$7.4 \cdot 10^{-6}$
	9	0.01174	1.07621	0.29910		0.99966	0.00179	$2.2 \cdot 10^{-5}$	$7.4 \cdot 10^{-6}$

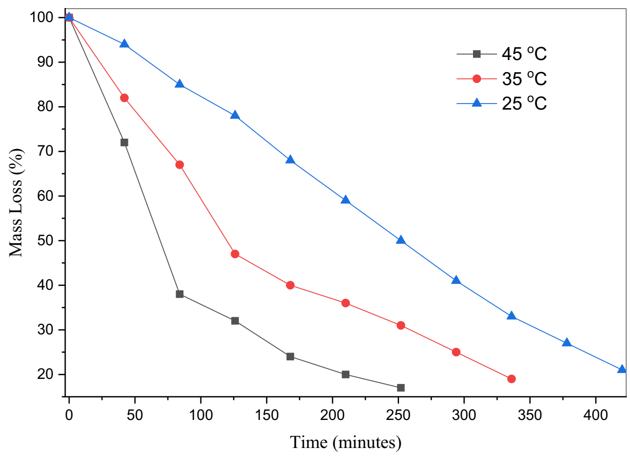

Fig. 4 Drying curves of the basil leaves at different temperatures of air at 1.5 m/s

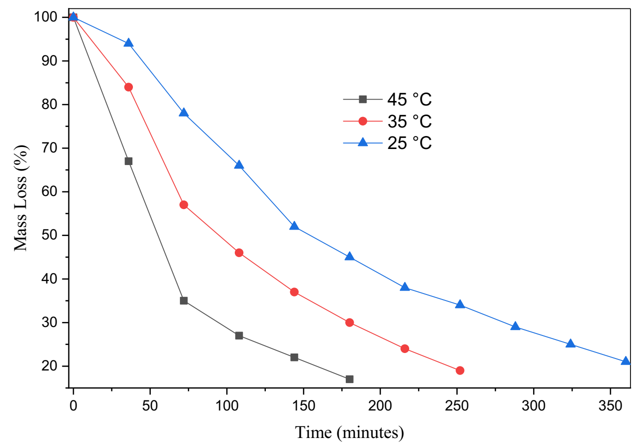

Fig. 6 Drying curves of the basil leaves at different temperatures of air at 3.0 m/s

energies in the constant drying region were found between 1 and 10 kJ/mol. In addition, it has been determined that the increase in temperature also increases the activation energy.

The drying process with the convection system was carried out at different temperatures (25 °C, 35 °C, and 45 °C) and different airflow rates (1.5 m/s, 2.25 m/s, and 3.0 m/s). It is seen in Fig. 4 that the drying time was maximum at both low air flow rate and low temperature.

As seen in Figs. 5 and 6, the drying time decreased as the temperature increased with the flow rate of air. In the drying process, the leaves of the basil vegetable can be dried as much as the equilibrium moisture amount carried by air at a certain temperature.

Under natural conditions, Arapgir basil leaves lose 80% of their mass at room temperature in about a week. As seen in Fig. 7, the evaporation rate of moisture in the first 4-day period with natural convection can be expressed by a decreasing curve equation. In the following days, the evaporation rate of moisture slowed down and reached the equilibrium humidity of the air.

As seen in Fig. 8, the evaporation rate of moisture in the basil leaf is directly proportional to both the temperature and the flow rate of the air. The drying process with forced convection takes place much faster than natural convection. The parameters affecting the evaporation rate can be listed as the surface area of the leaf, the humidity of the air, the flow rate, and the temperature of the air.

3.3 Evaluation of drying kinetics with RSM

In this study, an experimental design was made with statistical regression according to RSM method, and optimum conditions were determined according to response functions. In experimental design, it is necessary to determine the effective parameters to find optimum results with a small number

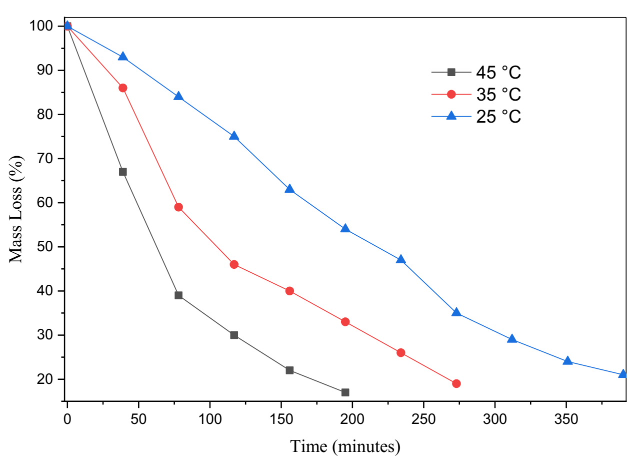

Fig. 5 Drying curves of the basil leaves at different temperatures of air at 2.25 m/s

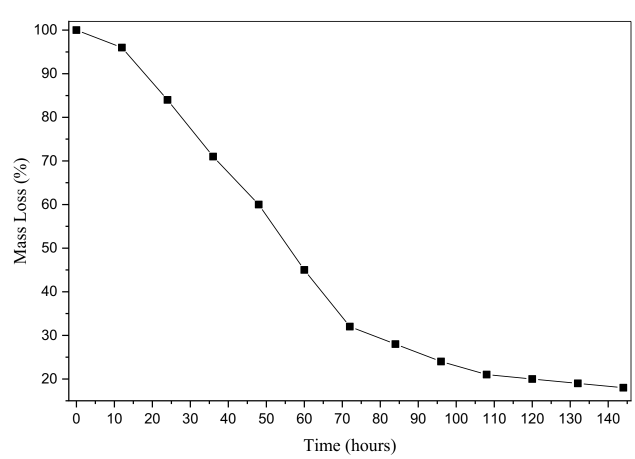

Fig. 7 Drying Arapgir basil under the natural conditions with the help of sunlight at nearly 25 °C

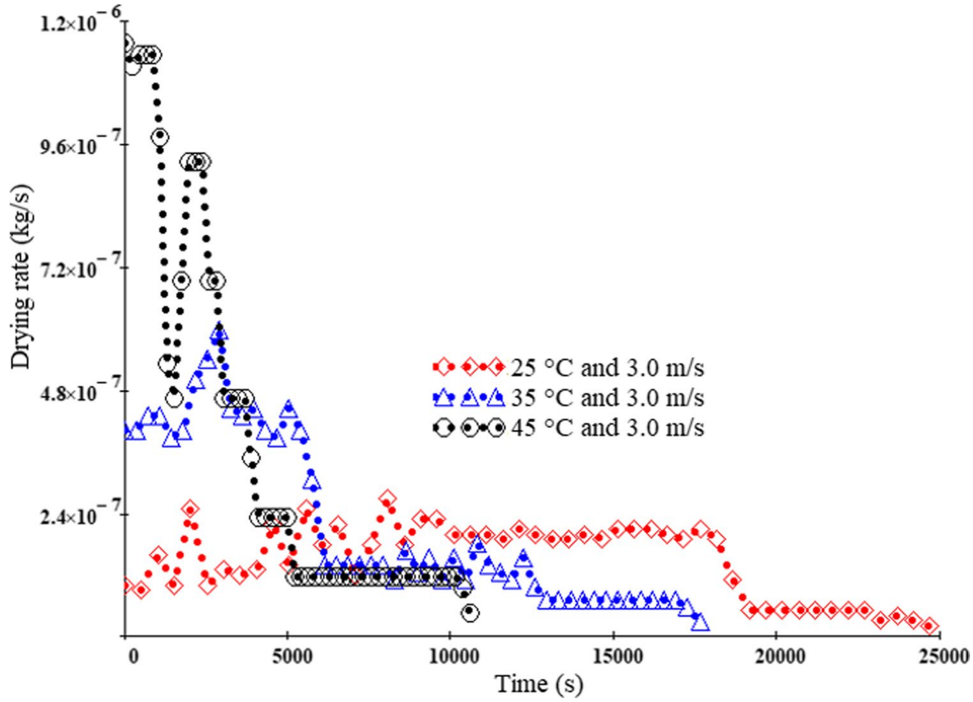

Fig. 8 The rate of moisture evaporation over time at different flow rates and different temperatures of Arapgir basil leaves per unit area

of experiments. The response functions of these parameters in the process are evaluated statistically in a fast and reliable way, and a solution is reached. According to the RSM method, the most appropriate results are obtained in the most economical, short time, and with maximum efficiency by consuming less energy. Similar RSM design and experimental optimizations have been used in studies on drying kinetics of plant leaves. Comparisons were made by evaluating the experimental and theoretical model results obtained with a statistical approach [28–31].

In Fig. 9, the effect of airflow rate and temperature on the drying time is given according to the results of RSM. In Table 7, statistical analysis values of the most suitable models are given. With the approach obtained in natural logarithmic Eq. 15, the closest results to the experimental values were modeled (Fig. 10).

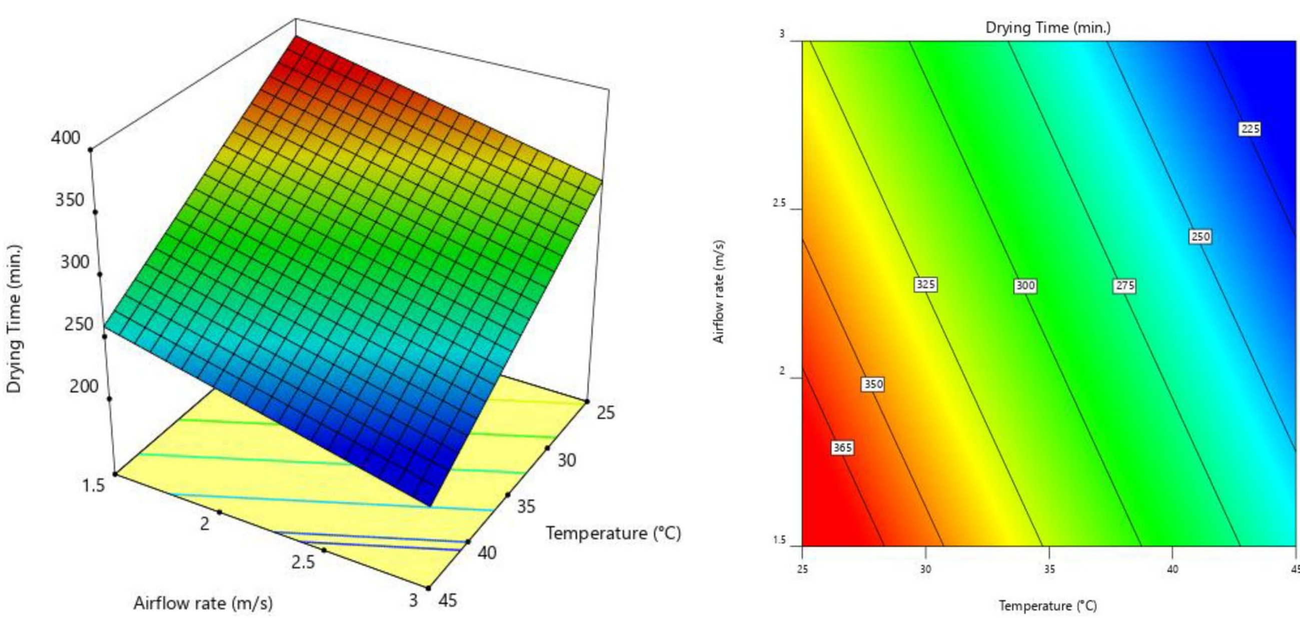

Fig. 9 RSM model of the drying time of Arapgir basil, which depends on airflow rate and temperature

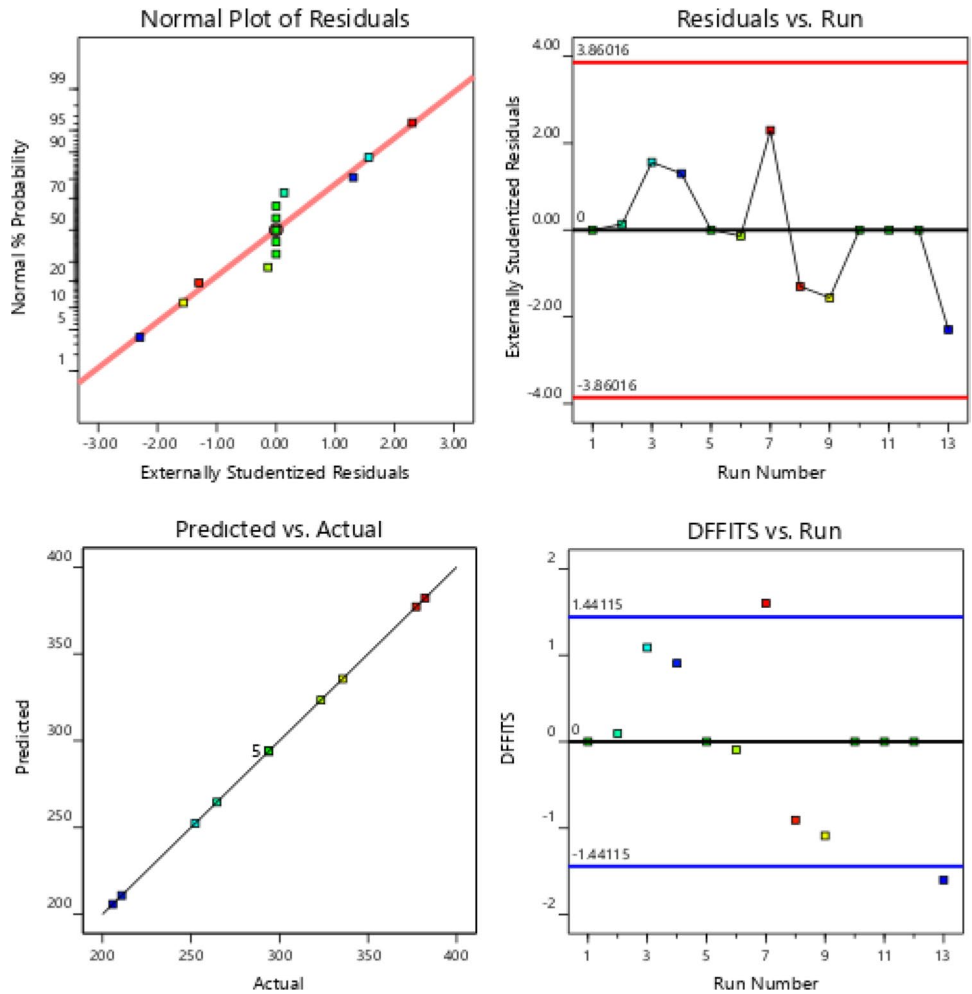

Fig. 10 Linear and regional distribution of experimental data according to the model according to the RSM statistical analysis

$$ln(t) = -0.000471 \cdot T^2 - 0.008760 \cdot v^2 - 0.004212 \cdot T \cdot v + 0.268564 \cdot T + 1.19984 \cdot v - 32.12951 \quad (15)$$

4 Conclusion

It is known that drying foods at high temperatures reduce their nutritional value. For this reason, the drying process was not carried out with convection and a PID-controlled system at high temperatures. Energy efficiencies in different processes were compared by performing an exergy analysis in the drying process. It has been observed that the energy consumed and lost especially in the convectional drying system (tray dryer) is very high. In the experiments conducted in the PID system, the lowest efficiency was found in the isothermal process.

The shrinkage behavior of Arapgir basil during drying has been determined according to the new improved model. It has been observed that the equation developed depending on the leaf width, length, and conversion ratio is compatible with both the experimental data and the models in the literature. Here, it is understood that the transformation rate directly affects the area and mass of the leaf.

Accordingly, the most suitable system in exergy efficiency has been determined as the non-isothermal system. Maximum energy loss and minimum exergy efficiency in the

Table 7 The most suitable models determined according to the RSM work plan and their statistical analysis

Transformation	Source	Sum of squares	Mean square	*F*-values	*P*-values	Std. dev	R^2	%C.V
Square root	Quadratic vs 2FI	0.0685	0.0342	756.58	0.0001	0.0067	0.9995	0.0394
Natural log	Quadratic vs 2FI	0.0039	0.0019	425.32	0.0001	0.0021	0.9996	0.0376

convection drying process were found at 45 °C temperature and 3.0 m/s airflow. Exergy efficiencies were calculated to be approximately 4% in convection, 26% in isothermal, and 32% in non-isothermal drying. The exergy efficiency of the system is very low as there is a lot of energy loss in convectional systems such as tray dryers. Especially in systems where energy losses are minimum, there is maximum exergy efficiency.

References

1. Altay K, Hayaloglu AA, Dirim SN (2019) Determination of the drying kinetics and energy efficiency of purple basil (Ocimum basilicum L.) leaves using different drying methods. Heat and Mass Transfer/Waerme- Und Stoffuebertragung, 55(8), 2173–2184. https://doi.org/10.1007/s00231-019-02570-9
2. Amini G, Salehi F, Rasouli M (2021) Drying kinetics of basil seed mucilage in an infrared dryer: application of GA-ANN and ANFIS for the prediction of drying time and moisture ratio. J Food Process Preserv 45(3):1–9. https://doi.org/10.1111/jfpp.15258
3. Calín-Sánchez Á, Lech K, Szumny A, Figiel A, Carbonell-Barrachina ÁA (2012) Volatile composition of sweet basil essential oil (Ocimum basilicum L.) as affected by drying method. Food Res Int, 48(1), 217–225. https://doi.org/10.1016/j.foodres.2012.03.015
4. Díaz-Maroto MC, Palomo ES, Castro L, González Viñas MA, Pérez-Coello MS (2004) Changes produced in the aroma compounds and structural integrity of basil (Ocimum basilicum L) during drying. J Sci Food Agric 84(15):2070–2076. https://doi.org/10.1002/jsfa.1921
5. El-Sebaii AA, Shalaby SM (2012) Solar drying of agricultural products: a review. Renew Sustain Energy Rev 16(1):37–43. https://doi.org/10.1016/j.rser.2011.07.134
6. Kadam DM, Goyal RK, Gupta MK (2011) Mathematical modeling of convective thin layer drying of basil leaves. Journal of Medicinal Plant Research 5(19):4721–4730
7. Orphanides A, Goulas V, Gekas V (2016) Drying technologies: vehicle to high-quality herbs. Food Engineering Reviews 8(2):164–180. https://doi.org/10.1007/s12393-015-9128-9
8. Erbay Z, Hepbasli A (2014) Application of conventional and advanced exergy analyses to evaluate the performance of a ground-source heat pump (GSHP) dryer used in food drying. Energy Convers Manage 78:499–507. https://doi.org/10.1016/j.enconman.2013.11.009
9. Gungor A, Tsatsaronis G, Gunerhan H, Hepbasli A (2015) Advanced exergoeconomic analysis of a gas engine heat pump (GEHP) for food drying processes. Energy Convers Manage 91:132–139. https://doi.org/10.1016/j.enconman.2014.11.044
10. Hernández JA, Pavón G, García MA (2000) Analytical solution of mass transfer equation considering shrinkage for modeling food-drying kinetics. J Food Eng, 45(1), 1–10. https://doi.org/10.1016/S0260-8774(00)00033-9
11. Malekjani N, Jafari SM (2018) Simulation of food drying processes by computational fluid dynamics (CFD); recent advances and approaches. Trends Food Sci Technol 78:206–223. https://doi.org/10.1016/j.tifs.2018.06.006
12. Nagaya K, Li Y, Jin Z, Fukumuro M, Ando Y, Akaishi A (2006) Low-temperature desiccant-based food drying system with airflow and temperature control. J Food Eng 75(1):71–77. https://doi.org/10.1016/j.jfoodeng.2005.03.051
13. Shahi NC, Singh A, Kate AE (2014) Activation energy kinetics in thin layer drying of basil leaves. Int J Sci Res (IJSR) ISSN, 3(7), 1836–1840. www.ijsr.net
14. Picado A, Martínez J (2006) Cinética de Secado de la Levadura Cervecera (Saccharomyces cerevisiae). Nexo Revista Científica 19(1):49–56
15. Bennamoun L, Khama R, Léonard A (2015) Convective drying of a single cherry tomato: modeling and experimental study. Food Bioprod Process 94:114–123. https://doi.org/10.1016/j.fbp.2015.02.006
16. Londer BEB, Uzzard VAB, Imova IRS, Loat LIS, Oyle BRADB, Ipson REL, Eaucage BRAG, Ndrade ANA, Arber BEB, Arnes CHB, Ushey DHB, Artagena PAC, Haney MAXC, Ontreras KAC, Ox MAC, Ueto MAYAC, Urtis CAC, Isher MAF, Urst LIF, … Nquist BRJE (2012) The Leaf - area shrinkage effect can bias paleoclimate and aleoclimate and ecology Research1. 99(11), 1756–1763. https://doi.org/10.3732/ajb.1200062
17. Goula AM, Chasekioglou AN, Lazarides HN (2015) Drying and shrinkage kinetics of solid waste of olive oil processing. Drying Technol 33(14):1728–1738. https://doi.org/10.1080/07373937.2015.1026983
18. Aydoğmuş E, Arslanoğlu H (2021) Kinetics of thermal decomposition of the polyester nanocomposites. Pet Sci Technol 39(13–14):484–500. https://doi.org/10.1080/10916466.2021.1937218
19. Linghu R, Zhang Y, Zhao M, Huang L, Sun G, Zhang S (2019) Combustion reaction kinetics of char from in-situ or ex-situ pyrolysis of oil shale. Oil Shale 36(3):392–409. https://doi.org/10.3176/oil.2019.3.03
20. Khawam A, Flanagan DR (2006) Solid-state kinetic models: basics and mathematical fundamentals. J Phys Chem B 110(35):17315–17328. https://doi.org/10.1021/jp062746a
21. Aghbashlo M, Mobli H, Rafiee S, Madadlou A (2013) A review on exergy analysis of drying processes and systems. Renew Sustain Energy Rev 22:1–22. https://doi.org/10.1016/j.rser.2013.01.015
22. Gulcimen F, Karakaya H, Durmus A (2016) Drying of sweet basil with solar air collectors. Renewable Energy 93:77–86. https://doi.org/10.1016/j.renene.2016.02.033
23. Karthikeyan AK, Murugavelh S (2018) Thin layer drying kinetics and exergy analysis of turmeric (Curcuma longa) in a mixed mode forced convection solar tunnel dryer. Renewable Energy 128:305–312. https://doi.org/10.1016/j.renene.2018.05.061
24. Ravula SR, Munagala SR, Arepally D, Ravula PR, Golla S (2017) Mathematical modelling and estimation of effective moisture diffusivity and activation energy, exergy analysis of thin layer drying of pineapple. J Experiment Biol Agricult Sci, 5(2), 390–401. https://doi.org/10.18006/2017.5(3).392.401
25. Arslan D, Musa Özcan M (2008) Evaluation of drying methods with respect to drying kinetics, mineral content and colour characteristics of rosemary leaves. Energy Convers Manage 49(5):1258–1264. https://doi.org/10.1016/j.enconman.2007.08.005
26. Gunhan T, Demir V, Hancioglu E, Hepbasli A (2005) Mathematical modelling of drying of bay leaves. Energy Convers Manage 46(11–12):1667–1679. https://doi.org/10.1016/j.enconman.2004.10.001
27. Orhan R, Aydoğmuş E, Topuz S, Arslanoğlu H (2021) Investigation of thermo-mechanical characteristics of borax reinforced polyester composites. Journal of Building Engineering 42(July):103051. https://doi.org/10.1016/j.jobe.2021.103051
28. Shirzad H, Niknam V, Taheri M, Ebrahimzadeh H (2017) Ultrasound-assisted extraction process of phenolic antioxidants from Olive leaves: a nutraceutical study using RSM and LC–ESI–DAD–MS. J Food Sci Technol 54(8):2361–2371. https://doi.org/10.1007/s13197-017-2676-7
29. Šumić Z, Vakula A, Tepić A, Čakarević J, Vitas J, Pavlić B (2016) Modeling and optimization of red currants vacuum drying process by response surface methodology (RSM). Food Chem 203:465–475. https://doi.org/10.1016/j.foodchem.2016.02.109
30. Şahin S, Elhussein E, Bilgin M, Lorenzo JM, Barba FJ, Roohinejad S (2018) Effect of drying method on oleuropein, total phenolic

content, flavonoid content, and antioxidant activity of olive (Olea europaea) leaf. J Food Process Preserv, 42(5). https://doi.org/10.1111/jfpp.13604

31. Şen FB, Aşçı YS, Bekdeşer B, Bener M, Apak R (2019) Optimization of microwave-assisted extraction (MAE) for the isolation of antioxidants from basil (Ocimum basilicum L.) by response surface methodology (RSM). Anal Lett, 52(17), 2751–2763. https://doi.org/10.1080/00032719.2019.1600531